

# Pareto set analysis: local measures of objective coupling in multiobjective design optimization

Bart D. Frischknecht · Diane L. Peters ·  
Panos Y. Papalambros

Received: 14 May 2010 / Revised: 7 September 2010 / Accepted: 1 November 2010 / Published online: 24 November 2010  
© Springer-Verlag 2010

**Abstract** Multiobjective optimization focuses on the explicit trade-offs between competing criteria. A particular case is the study of combined optimal design and optimal control, or co-design, of smart artifacts where the artifact design and controller design objectives compete. In the system-level co-design problem, the objective is often the weighted sum of these two objectives. A frequently referenced practice is to solve co-design problems in a sequential manner: design first, control next. The success of this approach depends on the form of coupling between the two subproblems. In this paper, the coupling vector derived for a system problem with unidirectional coupling is shown

to be related to the alignment of competing objectives, as measured by the polar cone of objective gradients, in the bi-objective programming formulation. Further, it is shown that a measure describing the case where a range of objective weighting values for the system objective result in identical design solutions can be normalized when the system problem is considered as a bi-objective one. Changes to the mathematical structure and input parameter values of a bi-objective programming problem can lead to changes in the shape of the attainable set and its Pareto boundary. We illustrate the link between the coupling and alignment measures and the outcomes of the Pareto set. Systematically studying changes to coupling and alignment measures due to changes to the multiobjective formulation can yield deeper insights into the system-level design problem. Two examples illustrate these results.

An earlier version of this manuscript was published as Frischknecht, B., Peters, D., Papalambros, P., 2009, Pareto Set Analysis: Local Measures of Objective Coupling in Multi-objective Design Optimization, The 8th World Congress on Structural and Multidisciplinary Optimization, Lisbon, Portugal, June 1–5, Paper No. 1158.

This research was partially supported by the Ford Motor Company–University of Michigan Innovation Alliance, the Automotive Research Center, a US Army RDECOM Center of Excellence headquartered at the University of Michigan, Graduate Fellowships by the Rackham Graduate School at the University of Michigan, and by NSF grant #0625060.

B. D. Frischknecht (✉)  
Centre for the Study of Choice, University of Technology Sydney,  
645 Harris St, Level 4, Ultimo, NSW, 2007, Australia  
e-mail: bart.frischknecht@uts.edu.au

D. L. Peters · P. Y. Papalambros  
Mechanical Engineering, University of Michigan,  
2250 G.G.Brown, 2350 Hayward Street,  
Ann Arbor, MI 48105, USA

D. L. Peters  
e-mail: dlpeters@umich.edu

P. Y. Papalambros  
e-mail: pyp@umich.edu

**Keywords** Pareto set · Sensitivity analysis · Co-design · Objective coupling · Design optimization · Multiobjective optimization

## Nomenclature

$\Gamma_v$	Coupling vector comparing artifact and system objectives
$\Phi$	Constraint decoupling ratio
$\alpha$	Angle between two objective gradients
$\beta$	Angle between system level objective gradient directions for which $\mathbf{x}^*$ is the solution to the system design problem
$\gamma$	Lagrange multipliers for inequality constraints
$\eta_1$	Weighting factor in bi-objective minimization problem

$\eta_2$	Weighting factor in bi-objective minimization problem	$\mathbf{p}$	Fixed value parameters
$\theta^<$	Polar cone angle between two objective gradients	$r$	Pulley radius
$\lambda$	Lagrange multipliers for equality constraints	$s$	Frequency domain variable in Laplace transform
$\mu$	Coefficient of friction for power screw	$t_s$	Settling time
$\mathcal{A}$	Attainable set of objective vectors	$w_1$	Artifact objective weight
$\mathcal{X}$	Feasible design domain	$w_2$	Controller objective weight
$A$	State coefficient matrix determining the unforced system response	$\mathbf{x}_1$	Artifact design variables
$B$	State coefficient matrix determining the forced system response	$\mathbf{x}_2$	Controller design variables
$C$	Vector determining example system output from system states	$\mathbf{x}^*$	Vector of design variables that produces a nondominated set of objective values
$E$	Control effort over a set interval of time	$\nabla f_i$	Gradient of the objective function $i$
$G$	Precompensator in controller	$\nabla f_2^n$	Gradient of the nested controller objective function
$M$	Mass connected to a fixed surface by a linear spring		
$M_p$	Overshoot in the position response of the mass		
$K_1$	Controller state feedback gain associated with position		
$K_2$	Controller state feedback gain associated with velocity		
$\mathbf{Q}^<(\mathbf{x})$	The set of points that are superior to a particular $\mathbf{x}$		
$\mathbf{Q}^{\geq}(\mathbf{x})$	The set of points that are equal or inferior to a particular $\mathbf{x}$		
$\mathbf{Q}^{\sim}(\mathbf{x})$	The set of points that cannot be compared to a particular $\mathbf{x}$		
$R_a$	Armature resistance for DC motor		
$W$	Weighting factor used in coupling vector $W = w_2   w_1 = 1$		
$Z$	The displacement of the mass from its original position		
$c_1$	Constant based on material strength of spring		
$d_m$	Power screw diameter		
$f_1$	Artifact objective		
$f_2$	Controller objective		
$f_i^\circ$	Optimal objective value for criterion $i$ optimized singly		
$f_i^N$	Worst value of objective $i$ that is a member of Pareto set		
$\mathbf{f}^\circ$	Vector of ideal values for all criteria		
$\mathbf{x}^{f_i^\circ}$	Design variable vector that minimizes objective $i$ singly		
$\mathbf{g}_1$	Artifact inequality constraints		
$\mathbf{g}_2$	Controller inequality constraints		
$\mathbf{h}_1$	Artifact equality constraints		
$\mathbf{h}_2$	Controller equality constraints		
$\mathbf{k}$	An $n$ -dimensional vector with origin at $\mathbf{x}$ that lies within the polar cone of the two objective gradients		
$k_1, k_2$	Vectors representing the boundaries of the polar cone between two objective functions		
$k_s$	Linear spring constant		
$k_t$	Motor constant for DC motor		
$l$	Pitch length for power screw		

## 1 Introduction

The design of modern smart products requires concurrent optimization of the artifact design and its controller. This so-called co-design problem (Ou and Kikuchi 1996; Fathy et al. 2001; Reyer et al. 2001) is often performed in a sequential manner for reasons of convenience and tradition: design the artifact first, and then design its controller (Li et al. 2001; Chen and Cheng 2006). In general, such a strategy will yield non-optimal solutions, compared with a simultaneous or all-in-one optimization of the combined system (Fathy et al. 2001; Reyer et al. 2001), particularly when bi-directional coupling exists between the two subproblems, for example, when each of the two objectives depends on some variables and parameters of the other subproblem (Reyer et al. 2001). However, there exists a large class of problems where coupling is unidirectional. For example, the artifact criterion  $f_1(\mathbf{x}_1)$  depends only on the artifact design variables  $\mathbf{x}_1$  while the control criterion  $f_2(\mathbf{x}_1, \mathbf{x}_2)$  depends on both  $\mathbf{x}_1$  and the controller design variables  $\mathbf{x}_2$ , so that the system design objective becomes:

$$F = w_1 f_1(\mathbf{x}_1) + w_2 f_2(\mathbf{x}_1, \mathbf{x}_2), \quad (1)$$

where  $w_1, w_2$  are weights. Criteria interdependence, or coupling, can be measured by the partial derivatives of the artifact objective and constraint functions with respect to the controller variables when the artifact criterion is independent of the controller variables. A design example characterized by such a formulation is a linear positioning device where the artifact objective is steady-state displacement and the controller objective is settling time.

Partitioning artifact and controller variables may be desirable for practical purposes in cases where the effect of the controller variables on the artifact criterion is deemed small enough, or where the analytical or computational means are not available to treat artifact and control variables simultaneously for the controller objective. One strategy for the

latter case is to solve the system-level problem as a nested optimization one (Reyer et al. 2001; Fathy 2003), where the system solution is found with respect to  $\mathbf{x}_1$ , with the optimal  $\mathbf{x}_2$  computed as a function of  $\mathbf{x}_1$  by solving the “inner” optimal controller problem first (Fathy et al. 2001; Fathy 2003). This nested problem formulation is distinguished from the simultaneous one (1), using the notation

$$F^n = w_1 f_1(\mathbf{x}_1) + w_2 f_2^n(\mathbf{x}_2^*(\mathbf{x}_1)). \tag{2}$$

Figure 1 is a schematic illustrating the computational difference between a simultaneous and a nested optimization approach.

A limitation of the linear weighted criteria method is that it cannot find Pareto points in a non-convex region of the Pareto frontier (Das and Dennis 1997). Generalized weighted criteria methods consider functions in the place of constant weighting parameters (Athan and Papalambros 1996) and overcome the difficulty with non-convex Pareto frontiers. We preserve the weighted sum formulation for the system objective for simplicity and for interpretation in the context of previous co-design and control work.

One can view the co-design problem as a bi-objective Pareto formulation without scalarization and weights (whether or not we solve the controller objective as a nested problem),

$$\mathbf{F} = \begin{bmatrix} f_1(\mathbf{x}_1) \\ f_2(\mathbf{x}_1, \mathbf{x}_2) \end{bmatrix}. \tag{3}$$

We can retrieve a range of efficient solutions and thereby examine how much the two objectives compete or are aligned (Cohon 1978) as measured by the differences in the objective values or the design variables at different Pareto solutions. Intuitively, it would appear that objective alignment should relate to objective coupling.

Rather than taking the artifact and controller problem formulation as fixed, considering how the Pareto set as a

whole changes with changes in the problem formulation can facilitate the choice of problem formulation, in other words the choice of the attainable set, in addition to illustrating the tradeoffs between specific solutions. The design of the solution set rather than a single-point design is important in many design scenarios. Design scenarios of particular relevance share a characteristic that all design decisions are not made simultaneously, but some may be made before others (e.g., configuration design), some decisions may be more flexible than others, or be repeated at a higher frequency (e.g., dynamic controls, product platforming, design for adjustability), and some decisions, or exogeneities, may be uncertain (e.g., robust design, product development investment planning, regulatory policy).

In what follows, we show how a measure of objective alignment (the polar cone of objective gradients) is related to the coupling vector derived for a problem with unidirectional coupling. We also show how the measure of constraint decoupling can be normalized when the system design problem is considered as a bi-objective problem. Constraint decoupling occurs when, due to problem constraints, the system optimal design solution is identical over a range of weighting values for the individual criterion composing the system objective. These measures help to understand how the Pareto set is affected by changes to the system design problem formulation.

For an example application, consider the problem of designing a linear positioning device. Before the designer resolves the tradeoff of steady-state displacement versus settling time, she must first select whether the device is composed of a motor, drive belt, and pulley or a motor and power screw. We expect that this design topology choice will result in different Pareto set solutions for displacement and settling time. However, when making the choice between topologies, the designer is not concerned only with the displacement and settling time but also with the size, cost, reliability, and adaptability of the design. We illustrate how studying the coupling and alignment relationship for each topology can inform a designer’s topology decisions while reducing computational cost by not generating complete Pareto set representations. The proposed method is a suite of post-optimality analysis tools that can be employed to consider the tradeoffs between design objectives not only for one problem formulation, i.e., Pareto frontier, but across multiple problem formulations. Such analysis is particularly useful for cases where generating numerous Pareto optimal points to describe multiple Pareto frontiers is computationally expensive.

We use the combined design and control problem for the linear positioning system to illustrate the methodology for comparing different Pareto set solutions of the same problem. However, the methods can apply to a general class of problems that are characterized by asynchronous design

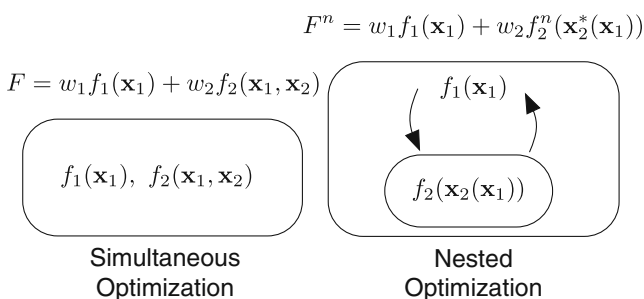


**Fig. 1** Schematic showing the difference between a simultaneous optimization and a nested one each with two subproblems  $f_1$  and  $f_2$

decision making. The first set of decisions is represented by a family of unique problem formulations, i.e., instances of (3). The second set of decisions is represented by the Pareto set of solutions for one of the unique problem formulations. The design objective is then to select the best problem formulation rather than the best design for a given problem formulation (Zeleny 1998).

There are at least three asynchronous design decision-making scenarios. First is the case where some decisions are made before others. For example, the design topology is selected before the final design can be specified in the case of the linear positioning system. Another example is the design of a product family where the product platform may be defined before the component designs are finalized (Nelson et al. 2001). Second is the case where initial decisions are made and then a second set of decisions is made repeatedly. An adjustable seat or a system with adaptive controls are examples of this scenario. Third is the case where there is uncertainty about the realization of a particular decision or external parameter (Levi et al. 2005). For example, the decision about the range of values for a part dimension can be made first by specifying a specific manufacturing process. The “decision” about the actual value of the design variable is made later when the product is produced. In another example, a structure could be designed to exhibit a particular natural frequency, but the decision about the load on the structure is made later given some external parameter such as wind velocity. Faced with each of these cases, it may be desirable for the designer considering the first set of design decisions to consider the range of solution possibilities, i.e., the Pareto set, with respect to the second set of decisions rather than a single “best” second decision given each first decision possibility.

This paper follows work related to the problem of comparing problem formulations or Pareto sets including the case where the change in the problem formulation is a change in a parameter value (Rao and Papalambros 1989; Rakowska et al. 1991), where the interest is to compare performance of different regions of the design space (Shan and Wang 2004), where the goal is to compare Pareto sets at different levels of robustness (Levi et al. 2005; Gunawan and Azarm 2005), and when the concern is about finding the overall shape of the Pareto set (Das 1999) or identifying specific regions of the Pareto set (Kasprzak and Lewis 2001).

Section 2 examines the relationship between objective alignment and objective coupling. Section 3 uses a numerical example to demonstrate the proposed Pareto set analysis and illustrate the terms introduced in Section 2. Section 4 presents a system co-design example that illustrates the relationship between the measures of objective alignment, coupling, and the Pareto set. Section 5 discusses how the Pareto set analysis can be used in design decision making.

## 2 Measures for comparing Pareto sets

Multiobjective programming typically focuses on finding Pareto points and defining the preference structure for selecting one point among many (Steuer 1986). A Pareto optimization problem is stated as:

$$\min_{\mathbf{x}} \mathbf{f}(\mathbf{x}; \mathbf{p}) \mid \mathbf{h}(\mathbf{x}; \mathbf{p}) = \mathbf{0}, \mathbf{g}(\mathbf{x}; \mathbf{p}) \leq \mathbf{0}, \mathbf{x} \in \mathcal{X} \quad (4)$$

Here  $\mathbf{f}(\mathbf{x}; \mathbf{p})$  is a vector of criteria of interest  $f_i$ ,  $i = 1, \dots, n$ . The set of variable values  $\mathbf{x}$  that satisfy all constraints is the feasible (design) domain,  $\mathcal{X}$ . The set of parameters  $\mathbf{p}$  take on fixed values. The set of all vectors  $\mathbf{f}$  mapped from the feasible domain is the attainable set  $\mathcal{A} = \{\mathbf{f}(\mathbf{x}; \mathbf{p}) \mid \mathbf{x} \in \mathcal{X}\}$ . A point in  $\mathcal{A}$ ,  $\mathbf{f}(\mathbf{x}^*; \mathbf{p})$ , is said to be non-dominated or Pareto optimal, if there exist no  $\mathbf{f}(\mathbf{x}; \mathbf{p})$  such that  $\mathbf{f}(\mathbf{x}; \mathbf{p}) \leq \mathbf{f}(\mathbf{x}^*; \mathbf{p})$  and  $f_i(\mathbf{x}; \mathbf{p}) < f_i(\mathbf{x}^*; \mathbf{p})$  for at least one  $i$ . Ideal values  $f_i^\circ$  are the optimal criterion values obtained optimizing one criterion at a time. The ideal or utopia point is the vector of ideal values for all criteria e.g.,  $\mathbf{f}^\circ = [f_1^\circ, f_2^\circ]'$ . A nadir value  $f_i^N$  is the worst value of  $f_i$  that is a member of the Pareto set.

One research area in multiobjective design optimization has been methods to aid the design decision maker in navigating the tradeoff between competing objectives. For example, Tappeta and Renaud used local sensitivity and second-order information around a particular Pareto point to develop an approximation of the Pareto frontier that could then be used as part of an iterative tradeoff exploration tool (Tappeta and Renaud 2001). Zhang et al. applied a similar approach to a robust design problem, and they emphasized the quadratic approximation of the Pareto surface as a candidate representation of the designer’s utility function or preference structure (Zhang et al. 2000). Kitayama et al. used the tradeoff matrix from Tappeta and Renaud (2001) to propose an automated iterative Pareto frontier exploration (Kitayama et al. 2009). Lootsma examined how the Pareto frontier relates to sensitivity in the objective functions (Lootsma 1999).

Several researchers have applied local Pareto front information beyond tradeoff ratios by considering objective function gradient differences in order to compare Pareto solutions (Purshouse and Fleming 2003; Carlsson and Fuller 1995; Deng 2007). Additionally, analogies to postoptimal analysis in single objective problems have been proposed, particularly for vector objective linear programming (Kornbluth 1974; Gal and Leberling 1977). Others have also discussed the idea of comparing different Pareto sets using the concept of a meta-Pareto set, which includes all non-dominated criteria vectors selected from the union of all the individual Pareto sets under consideration (Athans and Papalambros 1996; Mattson and Messac 2003).

Past research incorporated local Pareto front information to inform the tradeoff for a given problem formulation or examine the Pareto boundary alone for multiple problem formulations. We incorporate local measures of the Pareto front while applying these measures to compare distinct problem formulations, namely multiple Pareto frontiers, rather than a single problem formulation. We adopt or define several measures related to multiobjective programming problems and consider how these measures change with changes in the problem formulation, and the attendant implications for the Pareto set.

### 2.1 Quantification of objective coupling and alignment

The interdependence of multiple objectives for a given system is critical to its design (Balling and Sobieszcanski-Sobieski 1996; Bloebaum et al. 1992; Hajela et al. 1990). Considering the system problem of combined artifact and controller design, the co-design problem with unidirectional coupling is formulated as (Fathy 2003)

$$\begin{aligned} \min_{\mathbf{x}_1, \mathbf{x}_2} \quad & w_1 f_1(\mathbf{x}_1) + w_2 f_2(\mathbf{x}_1, \mathbf{x}_2) \\ \text{subject to:} \quad & \mathbf{h}_1(\mathbf{x}_1) = \mathbf{0}; \mathbf{h}_2(\mathbf{x}_1, \mathbf{x}_2) = \mathbf{0} \\ & \mathbf{g}_1(\mathbf{x}_1) \leq \mathbf{0}; \mathbf{g}_2(\mathbf{x}_1, \mathbf{x}_2) \leq \mathbf{0} \end{aligned} \tag{5}$$

where  $f_1(\mathbf{x}_1)$  is the artifact objective function,  $f_2(\mathbf{x}_1, \mathbf{x}_2)$  is the controller objective function,  $\mathbf{x}_1$  and  $\mathbf{x}_2$  are vectors of artifact and controller design variables,  $\mathbf{h}_1$  and  $\mathbf{h}_2$  are the artifact and controller equality constraints,  $\mathbf{g}_1$  and  $\mathbf{g}_2$  are the artifact and controller inequality constraints, and  $w_1$  and  $w_2$  are the weights associated with the objective functions  $f_1$  and  $f_2$ , respectively. In previous work on co-design coupling, emphasis has been placed on comparing  $f_1$  to the weighted system objective  $w_1 f_1 + w_2 f_2$  through a coupling vector  $\Gamma_v$  rather than comparing  $f_1$  and  $f_2$  directly (Fathy 2003).

The  $\Gamma_v$  vector is derived as follows. Consider the nested system design problem from (2) where the asterisk denotes that the optimal values for  $\mathbf{x}_2$  have been found with respect to  $\mathbf{x}_1$ . The coupling vector  $\Gamma_v$  is derived from the Karush–Kuhn–Tucker (KKT) optimality conditions for the weighted-sum objective describing the system design problem, where  $W = w_2/w_1 = 1$ , and

$$\Gamma_v = W \left( \frac{\partial f_2}{\partial \mathbf{x}_1} + \frac{\partial f_2}{\partial \mathbf{x}_2^*} \frac{\partial \mathbf{x}_2^*}{\partial \mathbf{x}_1} \right) = W \nabla f_2^n(\mathbf{x}_1). \tag{6}$$

The inner term in (6) is the gradient of  $f_2^n(\mathbf{x}_2^*(\mathbf{x}_1))$  from (2).  $\Gamma_v$  is assumed to be a row vector.

Objective decoupling occurs when the inner term of  $\Gamma_v$ , or  $\nabla f_2^n(\mathbf{x}_1)$ , vanishes. Two objectives are then said to be

independent at the particular design point  $\mathbf{x}$  when  $\Gamma_v = \mathbf{0}$ . In this case the solution to the system problem can be found by solving the two single-objective problems,  $\min f_1$  and  $\min f_2$  (Fathy 2003).

The magnitude of the coupling vector is meant to indicate the degree of coupling. The coupling vector  $\Gamma_v$  is difficult to interpret because it is directly proportional to the subjective weighting value  $W$  and the units of measurement for the objective function  $f_2$ . Comparing the two objectives directly frees the designer from implying a scale  $W$ , or “exchange rate”, between objectives before studying the attainable set. One can also think of the interdependence or alignment of the objectives as a function of gradient direction only (not magnitude).

#### 2.1.1 Gradient direction

To explore the idea of gradient direction we consider the necessary conditions for a Pareto point in a bi-objective minimization problem (Kuhn and Tucker 1951) as in (4):

$$\eta_1 \nabla f_1(\mathbf{x}^*) + \eta_2 \nabla f_2(\mathbf{x}^*) + \lambda^\top \nabla \mathbf{h}(\mathbf{x}^*) + \gamma^\top \nabla \mathbf{g}(\mathbf{x}^*) = \mathbf{0} \tag{7}$$

$$\gamma \geq \mathbf{0}; \lambda \neq \mathbf{0}; \gamma^\top \mathbf{g}(\mathbf{x}^*) = \mathbf{0}; \mathbf{h}(\mathbf{x}^*) = \mathbf{0} \tag{8}$$

Comparing (7) and (8) to what would be the first-order optimality conditions for (5) we see that the co-design problem is a special case of the bi-objective problem where the weighting factors  $\eta_1, \eta_2$  were chosen a priori to be  $w_1, w_2$ . Comparing gradient directions rather than coupling magnitudes is one way to normalize the objective tradeoff discussion. However, it should be noted that it is still possible that the gradient direction is affected by the scale of the controller variables  $\mathbf{x}_2$  since they do not appear in the artifact objective function.

The decision space in a multiobjective problem can be partitioned into three disjoint sets with respect to a feasible point  $\mathbf{x}$  (Zadeh 1963; Cohon 1978): Points  $[\mathbf{x}_1, \dots, \mathbf{x}_n]^\top \in \mathcal{R}^n$  that are superior, in a set  $\mathbf{Q}^<(\mathbf{x})$ ; points that are equal or inferior, in a set  $\mathbf{Q}^\geq(\mathbf{x})$ ; and points that cannot be compared, in a set  $\mathbf{Q}^\sim(\mathbf{x})$ . The set  $\mathbf{Q}^<(\mathbf{x})$  is equivalent to the interior of the polar cone of the negative objective gradients

$$\mathbf{Q}^<(\mathbf{x}) = \{ \mathbf{k} \mid -\mathbf{k}^\top \nabla f^i > \mathbf{0}; i = 1, 2 \} \tag{9}$$

where  $\mathbf{k}$  is an  $n$ -dimensional vector with origin at  $\mathbf{x}$ . The angle between the boundaries of the polar cone can then be taken as a measure of objective function alignment at a particular  $\mathbf{x}$ . A polar cone angle of  $\pi$  corresponds to the

case where the gradients of both objectives at  $\mathbf{x}$  are parallel with the same signs, or aligned. A polar cone angle equal to  $\pi$  implies coincident improving directions for both objectives. The polar cone angle collapses to zero when objective gradients are parallel with reversed signs.

The polar cone has an appealing geometric interpretation in that the larger the polar cone angle the greater the region of simultaneously improving directions, or the greater the objective alignment. From the definition of polar cone in (9), the polar cone angle is

$$\theta^< = \arccos\left(\frac{\mathbf{k}_1 \cdot \mathbf{k}_2}{|\mathbf{k}_1||\mathbf{k}_2|}\right),$$

$$\{\mathbf{k}_1| - \mathbf{k}_1 \nabla f_1(\mathbf{x}) = 0; \mathbf{k}_2| - \mathbf{k}_2 \nabla f_2(\mathbf{x}) = 0\}. \tag{10}$$

A convenient way to identify the appropriate  $\mathbf{k}_1$  and  $\mathbf{k}_2$  for a problem with two design variables is to recognize that  $\mathbf{k}_1, \mathbf{k}_2$  should be orthogonal to  $-\nabla f_1, -\nabla f_2$  and in the plane defined by  $f_1$  and  $f_2$ . We preserve the polar cone measure for the  $n$ -dimensional case but calculate it directly from the objective gradients:

$$\theta^< = \pi - \alpha, \tag{11}$$

where

$$\alpha = \arccos\left(\frac{\nabla f_1 \cdot \nabla f_2}{|\nabla f_1||\nabla f_2|}\right). \tag{12}$$

For an unconstrained bi-objective programming problem, the polar cone angle is zero for all Pareto points. These points belong to the set  $\mathbf{Q}^{\sim}(\mathbf{x})$ . The case is somewhat different for constrained bi-objective problems. The polar cone angle will take values between zero and  $\pi$  and may vary across the Pareto set. Together, the polar cone angles between objectives at points along the Pareto set, and the differences between ideal and nadir values for each objective give insight into the interdependence of the objectives for the problem formulation under consideration.

### 2.1.2 Decision parity

Another notion of objective alignment that we call decision parity refers to the similarity in the decision to be made  $\mathbf{x}$ , in order to minimize each objective  $f_1$  and  $f_2$  singly. A relative measure of decision parity is the  $L_2$  norm of the design variables between objective ideal points  $\|(\mathbf{x}^{f_1^\circ} - \mathbf{x}^{f_2^\circ})\|_2$ . Complete parity requires that the identical set of variable values minimizes both objectives. A degenerate case of decision parity is when the objectives are independent.

### 2.1.3 Pareto frontier slope

The coupling vector  $\Gamma_v$  is related to the slope of the Pareto frontier of the bi-objective problem (Peters et al. 2009), where at a given Pareto-efficient point  $\mathbf{x}^*$

$$\frac{df_2^*}{df_1^*} = \frac{1}{W} \Gamma_v \frac{d\mathbf{x}_1}{df_1^*} = \nabla f_2^{n\top} \cdot (1/\nabla f_1). \tag{13}$$

### 2.2 Normalized constraint decoupling

Returning to the geometric interpretation of the weighted-sum objective, (1), in the design variable space, the sum of any two vectors with positive weighting factors (e.g.,  $\nabla F = (1 - w)\nabla f_1 + w\nabla f_2 | w \geq 0$ ) will be a new vector (e.g.,  $\nabla F$ ) that lies between the two original vectors assuming the same origin. The necessary conditions for the optimal system design problem imply that the gradient of the weighted-sum-objective can be formed by a convex combination of the gradients of the active constraints. Constraint decoupling exists when, at a given Pareto point for a system design problem with weight  $w_i$ , the span of the convex combination of active and tight constraints will similarly satisfy the necessary conditions for optimality for a system design problem with some other weighting factor  $w_j \neq w_i$ .

This situation is illustrated in Fig. 2 for a two-dimensional linear programming problem with system objective  $F = (1 - w)f_1 + wf_2$  with two inequality constraints  $g_1$  and  $g_2$ . The angle  $\beta$  measures the range of system objective gradient directions for which  $\mathbf{x}^*$  is the solution to the system design problem. The angle  $\alpha$  measures the angle between the two single objective gradients. The ratio  $\phi = \beta/\alpha$  is defined as the constraint decoupling ratio.

The constraint decoupling ratio  $\phi$  can be calculated at an ideal point ( $f_1^\circ$ ) by first calculating the angle  $\alpha$  between the

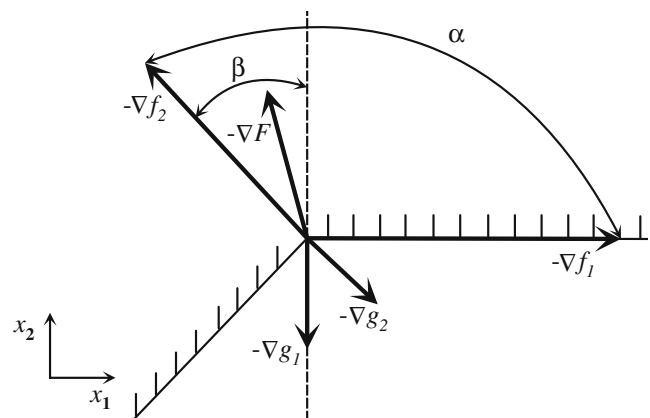


**Fig. 2** Constraint decoupling occurs in a scalarized multiobjective problem when a range of weighting values results in the same problem solution; shown here for linear functions

two single-objective gradients  $\nabla f_1, \nabla f_2$ . We can then find the limiting weighting value  $w^*$ , and compute the angle  $\beta$  between the weighted-sum system-objective gradient with weighting value  $w^*$  and  $\nabla f_1$ .

Assuming the system design objective is a convex combination of the single objectives, the limiting weighting value can be found by solving the following problem where  $\nabla f_1, \nabla f_2, \nabla \mathbf{g}, \nabla \mathbf{h}$  have been evaluated at  $(\mathbf{x}_1, \mathbf{x}_2)_{f_1^\circ}$ .

$$\begin{aligned} & \min_{w, \gamma, \lambda} \quad -w \\ \text{subject to:} & \quad (1-w)\nabla f_1 + w\nabla f_2 + \gamma^\top \nabla \mathbf{g} + \lambda^\top \nabla \mathbf{h} = \mathbf{0} \\ & \quad -\gamma \leq \mathbf{0}; \lambda \neq \mathbf{0} \end{aligned} \tag{14}$$

The ratio  $\phi$  evaluated at the ideal point  $f_1^\circ$  is then the ratio of the angle between the extreme weighted-sum objective gradient with the same optimal solution as the ideal point and the single-objective gradient  $\nabla f_1$ , and the angle between the two single-objective gradient vectors  $\nabla f_1$  and  $\nabla f_2$ :

$$\phi = \frac{\arccos\left(\frac{\nabla f_1 \cdot ((1-w^*)\nabla f_1 + w^*\nabla f_2)}{|\nabla f_1| |((1-w^*)\nabla f_1 + w^*\nabla f_2)|}\right)}{\arccos\left(\frac{\nabla f_1 \cdot \nabla f_2}{|\nabla f_1| |\nabla f_2|}\right)} = \frac{\beta}{\alpha} \tag{15}$$

The amount of constraint decoupling, or the range of weighting values for which the constraint decoupling conditions hold, will change with the objective scaling. However,  $\phi$ , based on the gradient directions will take a value between zero and one and will not change with objective scaling. A normalized measure can be defined for any Pareto point  $\mathbf{x}^*$  by replacing  $\nabla f_1$  in (14) with  $(1-\nu)\nabla f_1 + \nu\nabla f_2$ , where  $\nu$  is the minimum weighting value for which  $\mathbf{x}^*$  is the system design problem solution.

Constraint decoupling implies that, for the given problem formulation, there is a region of the attainable set where there exists a preference threshold. A designer’s preference for improvement in one objective must exceed a threshold value before she would incrementally move away from the current solution. A higher value of  $\phi$  represents a greater threshold. Given a fixed set of constraints, increasing objective gradient alignment will result in a higher  $\phi$ . Given a fixed set of objectives, decreasing satisfied-constraint gradient alignment will result in higher  $\phi$ .

### 3 Pareto set analysis

In the general case, systems characterized by multiple objectives will exhibit a tradeoff relationship between improvements for both objectives. Considering how the Pareto set as a whole changes with changes in the problem formulation can facilitate the choice of problem formulation, in other words the choice of the attainable set,

in addition to illustrating the tradeoffs between specific solutions.

The design of the solution set rather than a single-point design is important in many design scenarios. Design scenarios of particular relevance share a characteristic that all design decisions are not made simultaneously, but some may be made before others (e.g., configuration design), some decisions may be more flexible than others, or be repeated at a higher frequency (e.g., dynamic controls, product platforming, design for adjustability), and some decisions, or exogeneities, may be uncertain (e.g., robust design, product development investment planning, regulatory policy).

Changes to the mathematical structure and input parameter values of a bi-objective programming problem can lead to changes in the shape of the attainable set and its Pareto boundary. We illustrate the link between the terms described in Section 2 and outcomes of the Pareto set using a two-dimensional nonlinear programming example in Section 3.2, and a linear-positioning device design in Section 4.

#### 3.1 Problem specification and identification

The task of the designer, abstracted to a mathematical decision-making problem, is to specify the functional forms of the objective and constraint functions (referred to as system specification in the dynamic systems terminology), then partition model elements between parameters and variables, specify parameter values, and find efficient values for design variables (referred to as system identification in the dynamic systems terminology).

Each system specification and identification decision may affect the Pareto set. We classify changes to a system design problem formulation (summarized in Table 1) according to this definition of system specification and identification. For example, changing parameter values is equivalent to a traditional parametric study and fits in system identification. The examples listed in Table 1 reflect changes to the example problem specified in (16) below.

#### 3.2 Example

We now demonstrate examples of problem formulation changes and observe the corresponding changes to the Pareto set for a two-variable nonlinear programming problem modified from problem 10 in (Hock and Schittkowski 1981):

$$\begin{aligned} & \min [f_1 = 0.5x_1^2 - 7x_1, f_2 = x_2^2 - x_1x_2 - px_2]^\top \\ \text{subject to:} & \quad x_2^2 + 4x_1^2 - 25 \leq 0, p = 7 \end{aligned} \tag{16}$$

**Table 1** Classification of system design model changes

System modeling stage	Change	Example
Specification	Change objective functional form	–
	Change constraint functional form	–
	Add constraint	$x_2 - 5 + 2x_1 \leq 0$
	Remove constraint	–
	Repartition parameters and variables	–
Identification	Change parameter values	$p = 5$

**Table 2** Pareto set analysis results

Criterion	@	Case		
		a	b	c
Coupling vector ( $\Gamma_v, W = 1$ )	$f_1^\circ$	und.	und.	19
	$x_1 = 2.1$	8.66	2.47	14.2
	$f_2^\circ$	0	0	0
Polar cone angle ( $\theta^<$ )	$f_1^\circ$	$\pi/2$	$\pi/2$	$\pi/2$
	$x_1 = 2.1$	2.21	2.59	1.68
Sensitivity ( $df_2^*/df_1^*$ )	$f_2^\circ$	2.68	2.79	2.68
	$f_1^\circ$	und.	und.	-4.22
Constraint decoupling ( $\phi$ )	$x_1 = 2.1$	-1.77	-0.50	-2.90
	$f_2^\circ$	0	0	0
	$f_1^\circ$	0	0	0.29
	$x_1 = 2.1$	0	0	0
	$f_2^\circ$	0	0	0

The decision space of the problem is illustrated graphically in Fig. 3. Case (a) shows the unmodified problem, case (b) shows the case where  $p = 5$ , and case (c) includes the additional constraint  $x_2 - 5 + 2x_1 \leq 0$ . The objective gradients are shown for each case. Panel (d) shows the objective space where three Pareto points for each case are plotted. The slope of the Pareto front at each point is also plotted.

The ideal value  $f_1^\circ$  is found at  $\mathbf{x} = [2.5, 0]$  for all three cases. We compute the coupling vector, polar cone angle, slope of the Pareto front, and constraint decoupling ratio for each case evaluated at  $\mathbf{f}(\mathbf{x}^{f_1^\circ})$ . The values are reported in Table 2. The coupling vector and Pareto front slope are undefined for cases (a) and (b) given that the gradient for  $f_2$  is orthogonal to the gradient for  $f_1$ , i.e.  $\theta^< = \pi/2$ . At this particular point an improvement in  $f_2$  is achieved at no cost to  $f_1$ . For case (c) the polar cone angle does not change because the objective functions have not changed. However, due to the additional constraint, the feasible improving

direction for  $f_2$  changes, leading to a change in the coupling vector and Pareto front slope. Also due to the additional constraint, case (c) exhibits constraint decoupling at  $f_1^\circ$  with constraint decoupling ratio of 0.29. The dashed line in Fig. 3c shows the limiting gradient direction at  $f_1^\circ$  for which the system design problem will have the same solution as the single-objective problem  $f_1$ .

We can perform the same analysis for  $\mathbf{f}(\mathbf{x}^{f_2^\circ})$ . The solution is different for each case: (a)  $\mathbf{x} = [1.78, 3.52]$ ; (b)  $\mathbf{x} = [2.01, 2.96]$ ; (c)  $\mathbf{x} = [0.92, 3.17]$ . The coupling vector and Pareto front slope are zero for all three cases because an infinitesimal feasible improving step for  $f_1$  will yield no change for  $f_2$ . However, the polar cone angles are different between cases (a) and (b) reflecting that the change in parameter value  $p$  from 7 to 5 altered the orientation of

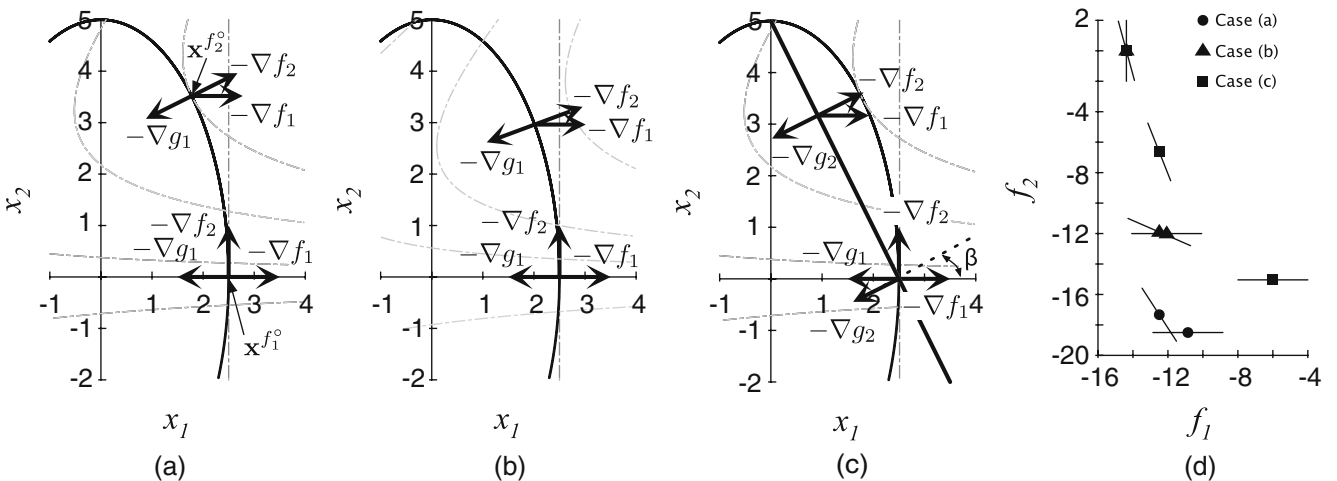


**Fig. 3** Graphical representation of problem given in (16) and modifications from Table 1. Panel a shows the unmodified problem. Panel b shows the case where  $p = 5$ . Panel c shows the case where the constraint  $x_2 - 5 + 2x_1 \leq 0$  has been added. Panel d plots points in the objective space for all three cases

$f_2$  so that the  $f_1$  and  $f_2$  objectives are more aligned in case (b) than in case (a).

A third point along the Pareto front is evaluated ( $x_1 = 2.1$ ) for each case. This point gives some sense for the overall shape of the Pareto front for each case. Evaluating the objectives at a fixed value of  $x_1$  is analogous in the co-design case to evaluating the system performance given a predefined artifact design with the best possible controller design for each case. The coupling vector, Pareto front slope, and polar cone angle are different across all three cases reflecting different levels of tradeoff between  $f_1$  and  $f_2$  and different levels of objective alignment. In this particular example, the cases are ordered consistently across all three metrics where an increase in magnitude of the coupling vector corresponds to an increasingly negative Pareto front slope and a decreasing polar cone angle.

Each Pareto point found in the example above increases the information available about the objective tradeoff. Computing the coupling vector, Pareto front slope, and polar cone angle at each point adds little computational burden while enhancing the overall description of the Pareto set. Examining Fig. 3d, case (a) is likely to dominate the other cases and so it may be judged superior if the range of performance criteria is the most important factor in the problem formulation selection. For reducing sensitivity of  $f_2$  with respect to  $f_1$ , case (b) would be superior when  $x_1 \approx 2.1$ .

### 4 System design example

We demonstrate the above Pareto set analysis for a simplified design and controls problem involving a positioning gantry. We consider two system topologies. In the first topology, shown in Fig. 4a, a mass  $M$  is connected to a fixed surface by a linear spring with constant  $k_s$ . A flexible belt connects the mass and a pulley with radius  $r$ , which

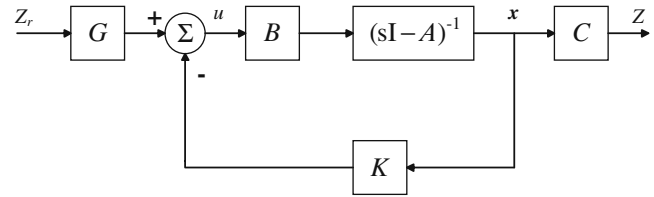


Fig. 5 Control architecture for linear positioning system

is mounted on a DC motor with armature resistance  $R_a$  and motor constant  $k_t$ . The displacement of the mass from its original position is  $Z$ . In the second topology, shown in Fig. 4b, the belt and pulley are replaced by a power screw with diameter  $d_m$ , coefficient of friction  $\mu$ , and pitch length  $l$ . A state-feedback controller with a precompensator is applied to the system, as shown in Fig. 5.

#### 4.1 Formulation

The optimization problem for both topologies is formulated as

$$\min_{M, k_s, K_1, K_2} F = w_1 f_1 + w_2 f_2 \tag{17}$$

$$f_1 = -Z_f(M, k_s) \tag{18}$$

$$f_2 = t_s(M, k_s, K_1, K_2) \tag{19}$$

subject to

$$g_1(M, k_s) = M - c_1 k_s^{2/3} \leq 0 \tag{20}$$

$$g_2(M, k_s, K_1, K_2) = M_p - M_{p, \max} \leq 0 \tag{21}$$

$$g_3(M, k_s, K_1, K_2) = E - E_{\max} \leq 0 \tag{22}$$

where  $c_1$  is a constant based on the material strength of the spring,  $M_p$  is the overshoot in the position response, and

Fig. 4 Linear positioning system

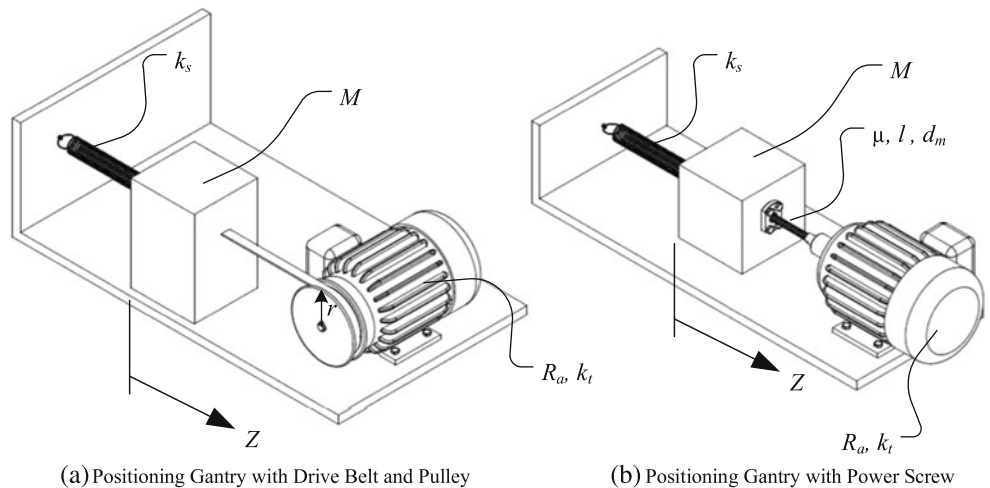


**Table 3** Parameters for gantry optimization

Parameter	$r$	$k_t$	$R_a$	$c_1$
Value	2.5 cm	10.0 N-m/A	2.0 kΩ	1.0
Parameter	$V_f$	$\mu$	$d_m$	$l$
Value	10 V	0.06	50 mm	10 mm

$E$  is the control effort over a set interval of time, calculated as  $E = \int_0^{t_f} (V(t))^2 dt$ .

Parameters used in the optimization are given in Table 3. Three points on the Pareto fronts for the two topologies are shown in Fig. 6, and a comparison of the Pareto measures is given in Table 4. Note that it is possible to evaluate the tradeoff present, despite the existence of only three Pareto points, which would normally present difficulties in visualizing and utilizing the Pareto frontier. For some measures, there is no difference between the two topologies. For example, neither exhibits constraint decoupling, and in both cases the polar cone angle  $\theta^< = \pi/2$  at all points along the Pareto set. There are some differences, however, which can be used to judge which topology might be desirable. It can be seen that the Pareto frontier corresponding to the first topology, with the belt drive, is dominant. Considering the slope of the Pareto front at point A indicates that the belt drive topology is less sensitive. This might also indicate that the belt drive is a better choice, if low sensitivity is considered desirable in the problem. The coupling vector  $\Gamma_v$ , however, has a smaller magnitude for the power screw topology for a number of points on the curve, including the point A. This might

**Table 4** Pareto set analysis results for positioning gantry

Criterion	Case		
	Belt drive	Power screw	
Coupling vector ( $\Gamma_v, W = 1$ )	$f_1^\circ$	[0 0]	[0 0]
	A	[-9.58 -11.81]	[-1.56 -1.89]
	$f_2^\circ$	und.	und.
Polar cone angle ( $\theta^<$ )	$f_1^\circ$	$\pi/2$	$\pi/2$
	A	$\pi/2$	$\pi/2$
	$f_2^\circ$	$\pi/2$	$\pi/2$
Sensitivity ( $df_2^*/df_1^*$ )	$f_1^\circ$	und.	und.
	A	-1.5	-9.5
	$f_2^\circ$	0	0
Constraint decoupling ( $\phi$ )	$f_1^\circ$	0	0
	A	0	0
	$f_2^\circ$	0	0

argue in favor of the power screw topology, if reducing the amount of coupling is of importance. The choice between these options will therefore depend on a full understanding of the design problem and what is considered to be important by the designer. Different circumstances will dictate the relevant Pareto set characteristics.

4.2 Computation

Figure 7 summarizes steps for computing the measures described above for analyzing the Pareto set for objective alignment and coupling (steps in the first large box), and for constraint decoupling (steps in the second large box). The coupling vector, the Pareto front slope, and the polar cone angle require the objective gradients  $\nabla f_1, \nabla f_2$  and the nested objective gradient  $\nabla f_2^n$ . The nested objective gradient is as follows  $\nabla f_2^n = \frac{\partial f_2}{\partial \mathbf{x}_1} + \frac{\partial f_2}{\partial \mathbf{x}_2^*} \frac{\partial \mathbf{x}_2^*}{\partial \mathbf{x}_1}$ , where the gradient  $\nabla f_2^n$  is computed in terms of  $\mathbf{x}_1$  assuming the optimal values  $\mathbf{x}_2^*$  given a particular  $\mathbf{x}_1$ .

It becomes necessary to compute gradients numerically in the case of an objective function described by a black box simulation or a function with difficult to compute gradients. The added computational cost to compute the gradients, and thereby compute the Pareto set analysis measures, is on the order of one optimization iteration compared to a minimum of several optimization iterations required to find an additional Pareto point. Pareto set analysis allows the designer to allocate computational budget to identify Pareto points from multiple problem formulations—e.g., various design topologies—rather than expending all resources to identify enough Pareto points in one problem formulation to describe the local behavior.

The numerical gradients may be sensitive to finite difference step size depending on the application. It is likely that this issue will be addressed by the designer when

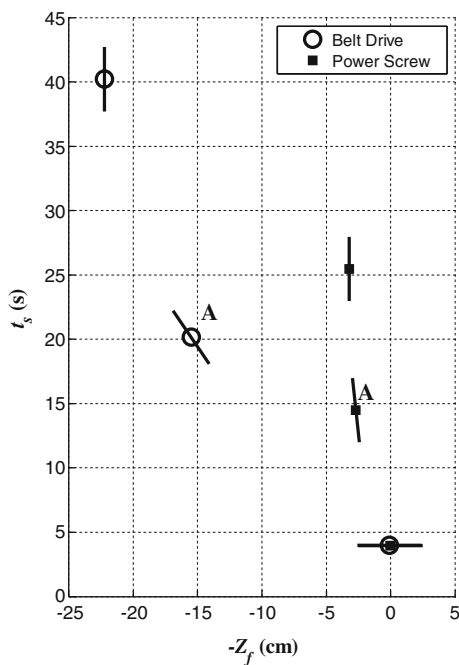
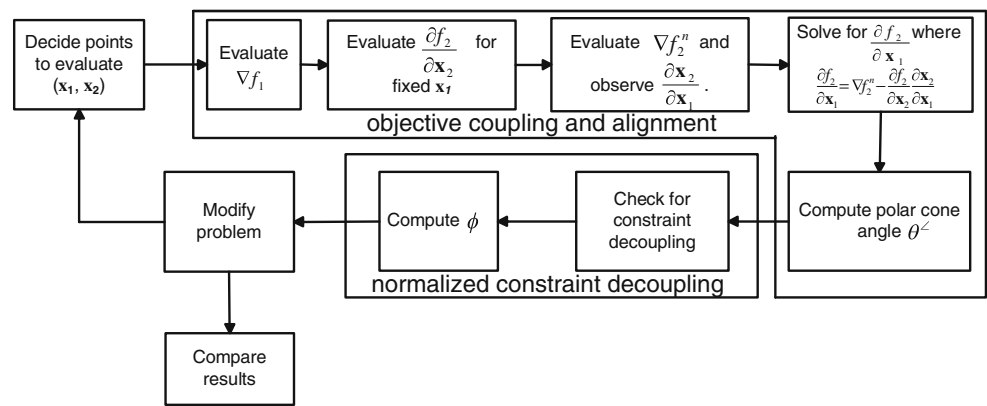


**Fig. 6** Comparison of Pareto frontiers for linear positioning device

**Fig. 7** Algorithm for evaluating objective alignment and coupling measures for multiple problem formulations



conducting optimization to find a Pareto point. The finite difference step size found to be suitable for optimization can be used to compute gradients for Pareto analysis. Methods for selecting appropriate finite difference step sizes are addressed by Barton (1992).

Objective coupling can be calculated analytically or numerically for a unidirectional coupled problem (2), following the definition in (6). Similarly, the polar cone angle can be calculated by evaluating the gradients for both objective functions. This is a straightforward process if the whole gradients are available:  $\nabla f_1(\mathbf{x}_1)$ ,  $\nabla f_2(\mathbf{x}_1, \mathbf{x}_2)$ . However, it can be challenging to formulate or compute the whole gradients when the controller objective is formulated as a nested problem with gradient  $\nabla f_2^n = \frac{\partial f_2}{\partial \mathbf{x}_1} + \frac{\partial f_2}{\partial \mathbf{x}_2} \frac{\partial \mathbf{x}_2^*}{\partial \mathbf{x}_1}$ . For example, assume  $f_2^n(\mathbf{x}_1)$  is a black-box simulation. We can then compute  $\nabla f_2^n(\mathbf{x}_1)$  and observe  $\partial \mathbf{x}_2^*/\partial \mathbf{x}_1$ . However, we require  $\nabla f_2(\mathbf{x}_1, \mathbf{x}_2)$ . If we assume we can compute  $\nabla f_2(\mathbf{x}_2)$  analytically or by evaluating the conventional controls problem  $f_2(\mathbf{x}_2)$ , then we can back out the missing component:  $\partial f_2/\partial \mathbf{x}_1 = \nabla f_2^n - \frac{\partial f_2}{\partial \mathbf{x}_2} \frac{\partial \mathbf{x}_2}{\partial \mathbf{x}_1}$ .

Computing the constraint decoupling ratio requires the objective gradients as well as solving the optimization problem described in (14) given a candidate design point. Suitable candidate design points are the ideal points  $f_1^\circ$  and  $f_2^\circ$  as well as points where constraint activity shifts. These interior constraint decoupling candidate points may not be easy to identify without solving for several Pareto points in order to find the constraint activity shifts. Therefore the computational costs to identify interior constraint decoupling may be high relative to the other measures.

Computing few Pareto points for each problem formulation and then computing the analysis measures is most advantageous for cases where objective functions are computationally expensive and there are numerous problem formulations to compare. For example, a designer may wish to compare various structural design topologies to compare vehicle mass versus crashworthiness. A single Pareto point could be found for each topology and the Pareto analysis measures could then be used to compare the tradeoff for

each topology. As resources are available, the designer can compute a second or third Pareto point and augment the analysis.

### 5 Discussion

A given design problem will exhibit varying tradeoffs between competing objectives depending on the problem formulation as illustrated in the numerical and system design example. In Section 1 we proposed that a designer’s criteria for selecting a given problem formulation frequently go beyond consideration of the explicit performance criteria represented in the bi-objective optimization problem. Some of these other considerations may be related to the structure of the tradeoff itself. For example, a designer may be willing to sacrifice performance capability for reduced sensitivity of the objectives to each other. The Pareto analysis measures can then be useful not only for describing the Pareto set when Pareto points are sparse, but also informing the designer on these other criteria.

Specifically, the designer may have a closed set of problem formulations, such as the belt and pulley or power screw configurations in Section 4, and then pick the problem formulation best suited to address the challenges of the design problem. Alternatively, the designer may use the information from the Pareto analysis to consider how the problem formulations might be changed in order to improve the tradeoff characteristics. There are three general means whereby the competition between objectives in a multiobjective problem can be reduced. First, a problem will exhibit reduced coupling between objectives when the partial gradients of the objective functions with respect to the shared design variables are reduced in magnitude. A special case is where the objectives can be solved as independent problems because there are no shared variables or the partial gradients with respect to the shared variables are zero at an optimal solution. Second, there is less difference between the optimal solution to both objectives when solved singly.

A special case is where a given design point is the minimizer for both objectives solved singly. Third, the problem can be constrained in such a way as to limit the feasible design space to regions where improvement in a direction for one objective occurs in the same direction as improvement for the other objective.

The polar cone angle can be evaluated at any point in the attainable set and gives a measure of objective alignment at that particular point. High polar cone angles within the attainable set suggest that there are regions of mutually improving directions. In contrast, high polar cone angles along the Pareto front could be an indication of an undesirable problem formulation in some design scenarios. Consider that in an unconstrained bi-objective problem, by definition the polar cone angle will be zero at all points along the Pareto set. High polar cone angles along the Pareto front may imply that the feasible design space is far away from both unconstrained objective optima. It should be noted that objective alignment on the Pareto front as measured by the polar cone of the objective gradients is different from a global notion of objective alignment that is perhaps best characterized by decision parity, or the differences in design variables between the two ideal points  $f_1^o, f_2^o$ .

Objectives that are highly aligned in terms of high polar cone angles on the Pareto front are then likely to be highly constrained. Reexamining the constraint formulation for the possibility to relax, reformulate, or eliminate constraints may be key to move toward improved objective values. Objective functions compete directly when polar cone angles along the Pareto front are low. Modifying objective functions through changes in design topology, parameter values, or other means may allow improvements in the objective function values.

The notion of Pareto front sensitivity is particularly useful for problems characterized by a primary objective and a secondary objective. For example, in a vehicle design problem with a safety objective such as maximize crashworthiness, a producer will primarily be concerned with improving the crashworthiness objective although other objectives such as vehicle mass may also be important. In this case it would be valuable to assess the local sensitivity, or incremental cost to the crashworthiness objective for decreases in vehicle mass. A designer may use the coupling vector, Pareto front slope, and polar cone angles in order to redesign the problem formulation to the benefit of both objectives or to the decreased sensitivity of one objective to the other. Depending on the Pareto analysis results these changes may be achieved best by a decrease in the coupling term due to constraint reformulation, objective reformulation, parameter/variable repartitioning, or modification of parameter values.

The Pareto set analysis described here can be conducted at any Pareto point regardless of how it was found. There-

fore we do not mean to imply that the linear weighted system design problem—posed for historical reasons from the co-design literature and for simplicity of exposition—be used to identify Pareto points. We describe the relationship between a scalar weighted sum objective and a bi-objective problem specifically to aid designers in considering a true multi-objective formulation rather than a single weighted sum objective with its corresponding difficulties.

With respect to the Pareto set analysis measures, the polar cone angle and the objective sensitivity, i.e. slope, are independent of weighting formulation. The coupling vector, which is the main criterion that we consider that relies on the weighted sum formulation, can be extended to other combinations of objectives including those that can identify points on a non-convex Pareto frontier (Peters 2010). The constraint decoupling ratio was derived from the KKT conditions for multiple objectives as originally described by Kuhn and Tucker (1951). Their formulation assumes a convex combination of objective functions. We leave for future work an extension to the constraint decoupling ratio similar to the extension for the coupling vector to non-convex Pareto points.

The focus of the paper is on bi-objective optimization due to its relevance to the co-design case and its prevalence across a broad range of optimization applications. Some extensions to more than two objectives are straightforward, and some extensions are left to future work.

The polar cone angle is a function of two objective gradients, which are defined in the design variable space. The region of mutually improving directions for all objectives  $1, \dots, n$  in the design space will be the empty set (and therefore the effective polar cone angle will be 0) unless one objective gradient can be described as a non-negative and non-zero convex combination of the other objective gradients:  $\nabla F_1 = \alpha[\nabla F_2 \nabla F_3 \nabla F_n]^T | \alpha > \mathbf{0}$ .

Polar cone angles can be computed for each pair of objective gradients and the smallest polar cone angle is taken as the effective polar cone angle for cases where a convex combination can be formed. The objective sensitivity or slope of the Pareto frontier can generalize to a gradient by selecting a baseline objective and computing the sensitivity of each other objective with respect to the baseline objective. The generalization of the coupling vector and the constraint decoupling ratio are left for future work.

## 6 Conclusions

We have shown how the particular case of co-design can be represented as a system design problem or alternatively as a bi-objective programming problem with an artifact objective and a controller objective. The coupling vector derived earlier for a system problem with unidirectional coupling

was shown to be related to the alignment of competing objectives, as measured by the polar cone of objective gradients, in the bi-objective programming formulation. We also showed how the measure of constraint decoupling can be normalized when the system problem is considered as a bi-objective one.

Systematically studying changes to coupling and alignment measures due to changes to the multiobjective formulation can yield deeper insights into the system-level design problem. We illustrated this approach with a simple nonlinear programming example and a positioning gantry co-design problem. The approach involves selecting one or several Pareto efficient points for analysis. These points can be evaluated for each change in problem formulation such as a change in the functional form of the objective function or a repartitioning of variables and parameters. Numerical measures were presented that describe each Pareto point in terms of the coupling between objectives, the sensitivity of one objective with respect to the other, the objective alignment and the extent of constraint decoupling. These measures can aid the designer seeking to reformulate the design problem to increase objective alignment or improve objective performance.

The desirability of a given Pareto set, or problem formulation, over another should be dictated by the design context. There are numerous design contexts where the designer is concerned with the attainable solution set and not only a point design solution. Such problems include the nested co-design problem described here and a wide variety of problems where the “control,” or partitioned variable design decisions, may be made asynchronously to the other design decisions.

As computational expense increases, it is not always feasible to generate a suitable graphical representation of the Pareto set. The methods presented in this paper provide a series of concrete steps to make the most out of a small number of analysis runs by connecting the local behavior of a bi-objective problem to the characteristics of the Pareto set. Future work may seek to extend the numerical measures described here to higher-dimension problems where graphical representation is similarly problematic.

**Acknowledgement** The opinions presented are solely those of the authors.

## References

- Athan TW, Papalambros PY (1996) Note on weighted criteria methods for compromise solutions in multi-objective optimization. *Eng Optim* 27(2):155–176
- Balling RJ, Sobieszcwanski-Sobieski J (1996) Optimization of coupled systems: a critical overview of approaches. *AIAA J* 34(1):6–17
- Barton RR (1992) Computing forward difference derivatives in engineering optimization. *Eng Optim* 20(3):205–224
- Bloebaum CL, Hajela P, Sobieszcwanski-Sobieski J (1992) Non-hierarchical system decomposition in structural optimization. *Eng Optim* 19(3):171–186
- Carlsson C, Fuller R (1995) Multiple criteria decision making: the case for interdependence. *Comput Oper Res* 22(3):251–260. doi:10.1016/0305-0548(94)E0023-Z
- Chen CY, Cheng CC (2006) 3d model based design for control of a mechatronic machine tools system. *Materials Science Forum: Progress on Advanced Manufacture for Micro/Nano Technology 2005* 505–507:967–972
- Cohon JL (1978) *Multiobjective programming and planning*. Academic, New York
- Das I (1999) On characterizing the “knee” of the Pareto curve based on normal-boundary intersection. *Struct Optim* 18(2–3):107–115
- Das I, Dennis JE (1997) Closer look at drawbacks of minimizing weighted sums of objectives for pareto set generation in multicriteria optimization problems. *Struct Optim* 14(1):63–69
- Deng H (2007) A similarity-based approach to ranking multicriteria alternatives. In: *Third international conference on intelligent computing, ICIC Aug. 2007. Advanced intelligent computing theories and applications. With aspects of artificial intelligence*. Springer-Verlag, Qingdao, China, pp 253–262
- Fathy HK (2003) *Combined plant and control optimization: theory, strategies and applications*. PhD Dissertation, Mechanical Engineering, University of Michigan, Ann Arbor
- Fathy HK, Reyer JA, Papalambros PY, Ulsoy AG (2001) On the coupling between the plant and controller optimization problems. In: *2001 American control conference, 25–27 June, vol 3. IEEE, Arlington, VA, pp 1864–1869*. doi:10.1109/ACC.2001.946008
- Gal T, Leberling H (1977) Redundant objective functions in linear vector maximum problems and their determination. *Eur J Oper Res* 1(3):176–184. doi:10.1016/0377-2217(77)90025-X
- Gunawan S, Azarm S (2005) Multi-objective robust optimization using a sensitivity region concept. *Struct Multidisc Optim* 29(1):50–60. doi:10.1007/s00158-004-0450-8
- Hajela P, Bloebaum CL, Sobieszcwanski-Sobieski J (1990) Application of global sensitivity equations in multidisciplinary aircraft synthesis. *J Aircr* 27(12):1002–1010
- Hock W, Schittkowski K (1981) *Test examples for nonlinear programming codes*. Springer-Verlag New York, Inc, Secaucus, NJ
- Kasprzak EM, Lewis KE (2001) Pareto analysis in multiobjective optimization using the collinearity theorem and scaling method. *Struct Multidisc Optim* 22(3):208–18. doi:10.1007/s001580100138
- Kitayama S, Yamazaki K, Arakawa M, Yamakawa H (2009) Quantitative trade-off analysis and its application to the compromise solution in the multi-objective design optimization. In: *8th world congress on structural and multidisciplinary optimization. ISSMO, Lisbon, Portugal*
- Kornbluth JSH (1974) Duality, indifference and sensitivity analysis in multiple objective linear programming. *Oper Res Q* 25(4):599–614
- Kuhn HW, Tucker AW (1951) *Nonlinear programming*. In: *Proceedings of the second Berkeley symposium on mathematical statistics and probability, 31 July–12 August 1950, University of California Press, Berkeley, CA, p 481*
- Levi F, Gobbi M, Mastinu G (2005) An application of multi-objective stochastic optimisation to structural design. *Struct Multidisc Optim* 29(4):272–284. doi:10.1007/s00158-004-0456-2
- Li Q, Zhang WJ, Chen L (2001) Design for control—a concurrent engineering approach for mechatronic systems design. *IEEE/ASME Trans Mechatron* 6(2):161–169
- Lootsma FA (1999) *Multi-criteria decision analysis via ratio and difference judgement*. Springer, New York
- Mattson CA, Messac A (2003) Concept selection using s-pareto frontiers. *AIAA J* 41(6):1190–1198

- Nelson II SA, Parkinson MB, Papalambros PY (2001) Multicriteria optimization in product platform design. *J Mech Des, Trans ASME* 123(2):199–204
- Ou JS, Kikuchi N (1996) Integrated optimal structural and vibration control design. *Struct Optim* 12(4):209–216
- Peters DL (2010) Coupling and controllability in optimal design and control. PhD Dissertation, Department of Mechanical Engineering, University of Michigan, Ann Arbor, Michigan
- Peters DL, Papalambros PY, Ulsoy AG (2009) On measures of coupling between the artifact and controller optimal design problems. In: 2009 ASME design engineering technical conference. ASME, San Diego, CA
- Purshouse RC, Fleming PJ (2003) Conflict, harmony, and independence: relationships in evolutionary multi-criterion optimisation. In: Proceedings evolutionary multi-criterion optimization. Second international conference, 8–11 April, Faro, Portugal, Springer-Verlag, pp 16–30
- Rakowska J, Haftka RT, Watson LT (1991) An active set algorithm for tracing parametrized optima. *Struct Optim* 3(1):29–44
- Rao JRJ, Papalambros PY (1989) Nonlinear programming continuation strategy for one parameter design optimization problems. In: Advances in design automation, vol 19-2, Univ of Michigan, Ann Arbor, MI, USA, Publ by American Soc of Mechanical Engineers (ASME), New York, NY, USA, Montreal, Que, Can, pp 77–89
- Reyer JA, Fathy HK, Papalambros PY, Ulsoy AG (2001) Comparison of combined embodiment design and control optimization strategies using optimality conditions. In: 2001 ASME design engineering technical conference. ASME, Pittsburgh, PA
- Shan S, Wang GG (2004) Space exploration and global optimization for computationally intensive design problems: a rough set based approach. *Struct Multidisc Optim* 28(6):427–441. doi:[10.1007/s00158-004-0448-2](https://doi.org/10.1007/s00158-004-0448-2)
- Steuer RE (1986) Multiple criteria optimization: theory, computation, and application. Wiley, New York
- Tappeta RV, Renaud JE (2001) Interactive multiobjective optimization design strategy for decision based design. *J Mech Des* 123(2): 205–215
- Zadeh LA (1963) Optimality and non-scalar-valued performance criteria. *IEEE Trans Automat Contr* AC-8(1):59–60
- Zeleny M (1998) Multiple criteria decision making: eight concepts of optimality. *Human Syst Manage* 17(2):97–107
- Zhang J, Wiecek MM, Chen W (2000) Local approximation of the efficient frontier in robust design. *J Mech Des, Trans ASME* 122(2):232–236. doi:[10.1115/1.533571](https://doi.org/10.1115/1.533571)